

AD-A136 104

ADA136104 TECHNICAL
LIBRARY

AD

TECHNICAL REPORT ARLCB-TR-83030

**BEHAVIOR OF PRESSURIZED CYLINDERS
WITH MULTIPLE INTERNAL CRACKS**

J. F. THROOP

F. FUJCAK

SEPTEMBER 1983



**US ARMY ARMAMENT RESEARCH AND DEVELOPMENT CENTER
LARGE CALIBER WEAPON SYSTEMS LABORATORY
BENÉT WEAPONS LABORATORY
WATERVLIET N.Y. 12189**

APPROVED FOR PUBLIC RELEASE; DISTRIBUTION UNLIMITED

DISCLAIMER

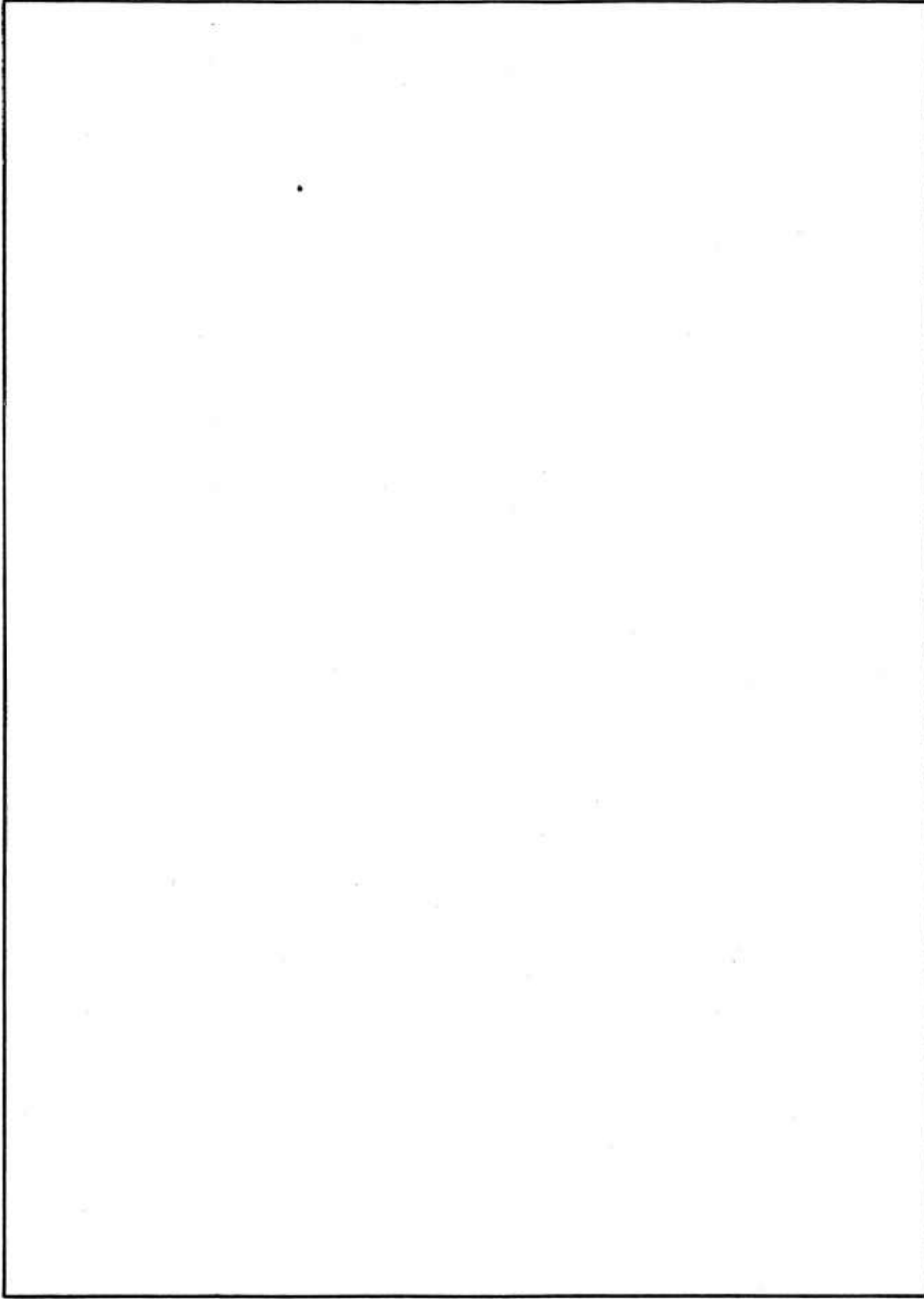
The findings in this report are not to be construed as an official Department of the Army position unless so designated by other authorized documents.

The use of trade name(s) and/or manufacturer(s) in this report does not constitute an official indorsement or approval.

DISPOSITION

Destroy this report when it is no longer needed. Do not return it to the originator.

SECURITY CLASSIFICATION OF THIS PAGE(When Data Entered)



SECURITY CLASSIFICATION OF THIS PAGE(When Data Entered)

TABLE OF CONTENTS

	<u>Page</u>
LIST OF SYMBOLS	iii
INTRODUCTION	1
OBJECT	1
THEORY	2
SPECIMENS, INSTRUMENTATION, AND PROCEDURE	4
SPECIMEN AM2437B	5
SPECIMEN AM3244B	6
SPECIMEN A2341B	6
SPECIMEN MB3244B	7
SPECIMEN B2341B	8
DISCUSSION	9
CONCLUSIONS	10
REFERENCES	11

LIST OF ILLUSTRATIONS

1. Crack depth, a , versus number of cycles.	12
2. Crack propagation rate versus crack depth, a .	13
3. Hoop strain versus crack depth.	14
4. Crack front shape change before failure.	15
5. Comparison of dual notches, 180 degrees apart after 1143 cycles.	16
6. Crack propagation rate versus crack depth for dual notches.	17
7. Comparison of hoop strain for dual notches.	18
8. Changes in shapes of crack #1 and crack #2 during last few cycles.	19

	<u>Page</u>
9. Crack depth versus number of cycles for four cracks.	20
10. Graph of da/dn versus crack depth for crack #1.	21
11. Hoop strain measured directly over four cracks.	22
12. Final shape of four cracks.	23
13. Crack depth versus number of cycles for dual notches, 30 percent overstrain.	24
14. da/dn versus crack depth for dual notches, 30 percent overstrain.	25
15. Hoop strain versus crack depth for dual notches, 30 percent overstrain.	26
16. Changes in shapes of crack #1 and crack #2 from dual notches, 30 percent overstrain, during final 200 cycles.	27
17. Crack depth versus number of cycles for dual notches, 60 percent overstrain.	28
18. da/dn versus crack depth for dual notches, 60 percent overstrain.	29
19. Hoop strain versus crack depth for dual notches, 60 percent overstrain.	30
20. Final crack shapes for dual notches, 60 percent overstrain.	31

LIST OF SYMBOLS

a	= crack depth
da/dn	= crack propagation rate
E	= modulus of elasticity
N	= fatigue cycles
N_f	= cycles for failure
P	= internal hydraulic pressure
%OS	= percent overstrain
R_a	= radius from center to crack tip
R_1	= inside radius
R_2	= outside radius
ϵ_0	= measured circumferential strain over the crack
ϵ_{th}	= theoretical circumferential strain at O.D. of uncracked cylinder
$\mu\text{in./in.}$	= microinch/inch
σ_o	= circumferential stress on outside surface
σ_i	= circumferential stress at the bore

INTRODUCTION

The strain behavior of thick-wall cylinders with a single fatigue crack grown from a longitudinal slot machined at the inner surface has been described previously.¹ It was shown that measurement of the strain on the outside surface directly over the crack gave an indication of how near the cylinder was to fatigue failure. It was found that as the crack deepens, the strain directly over the crack diminishes from the Lame' strain expected in an uncracked cylinder and approaches zero strain in a regular manner with increasing depth. When this strain reaches zero or becomes compressive the fracture of the cylinder is imminent. During this time the pressure within the crack is exerting a bending moment on the remaining ligament as well as adding to the circumferential tension; and the compressive strain on the outside of the ligament becomes greater than the circumferential tensile strain. When the remaining ligament finally becomes thin enough the tension in it once again exceeds the bending strains and stretches the ligament to failure causing failure of the cylinder. A plot of this strain versus crack depth may be used to anticipate the failure.

OBJECT

The object of this report is to show that the strain behavior of cylinders containing multiple notches or cracks is similar to the single notch case and may be analyzed the same way. A series of cylinders with 20 inch

¹Throop, J. F. and Fujczak, R. R., "Strain Behavior of Pressurized Cracked Thick-Walled Cylinders," Experimental Mechanics, The Society For Experimental Stress Analysis, August 1982, pp. 277-286.

(500 mm) long notches were tested. Three of them had two notches, 180 degrees opposed. One had zero percent overstrain (OS), one was subjected to 30 percent OS, and one was subjected to 60 percent OS. Also, one cylinder with four notches, 90 degrees apart, with zero percent OS was tested. For comparison the data for a cylinder with a single notch and zero percent OS is repeated from the earlier study.

The comparison of the dual notched cylinders will show the improvement in fatigue life brought about by autofrettage overstrain. The comparison of the single notch, dual notch, and quadruple notch will show if the dual notch is the worst case, as has been predicted analytically for the straight-fronted crack. Of course, these 20 inch (500 mm) long notches start off as straight-fronted cracks, but soon become semi-elliptical because they grow fastest at mid-length.

For each case, we present graphs of crack depth versus number of cycles, of crack rate versus crack depth, and of crack depth versus distance from the top of the specimen, as well as the graph of hoop stress versus crack depth.

THEORY

The stress and strain on the outside surface and the stress on the inside surface may be calculated by the following equations:²

$$\sigma_0 = P \frac{2R_1^2}{(R_2^2 - R_1^2)} \quad \text{on outside surface} \quad (1)$$

²Timoshenko, S. P. and Goodier, J. H., Theory of Elasticity, Third Edition, McGraw-Hill Book Company, New York, 1970, pp. 68-71.

$$\varepsilon_{th} = \frac{P}{E} \frac{2R_1^2}{(R_2^2 - R_1^2)} \quad \text{on outside surface} \quad (2)$$

$$\sigma_f = P \frac{(R_2^2 + R_1^2)}{(R_2^2 - R_1^2)} \quad \text{on outside surface} \quad (3)$$

An idealization presented by Shannon³ assumes wall thinning represented by an effective increase of the internal radius of the cylinder to include the deepest crack depth, with the pressure-bending effect applied as a moment on a section of depth equal to the remaining wall thickness of the cylinder. Thus, the equations for stress and strain on the outside surface of a cracked cylinder are as follows.

Uniform thinning and pressure-bending approximation for stress and strain in the cylinder with internal longitudinal straight-fronted crack of depth $a = (R_a - R_1)$:³

$$\sigma_0 = \frac{2PR_a^2}{(R_2^2 - R_a^2)} - \frac{3P(R_a - R_1)(R_2 - R_1)}{(R_2 - R_a)^2} \quad (4)$$

$$\varepsilon_0 = \frac{\sigma_0}{E} \quad (5)$$

This idealization gives the nature of the decrease in the strain directly over the crack. The actual decrease occurs more slowly with crack depth because the fatigue cracks do not remain straight-fronted.

³Shannon, R. W. E., "Crack Growth Monitoring by Strain Sensing," Pressure Vessels and Piping, (1), Applied Sciences Publishing Ltd., England, 1973, pp. 61-73.

SPECIMENS, INSTRUMENTATION, AND PROCEDURE

The strains on the external surface of 30 inch (0.76 m) long cylinders of high-strength steel were measured with bonded foil strain gages while pressurized in steps from zero to 48 ksi (330 MPa). The cylinders had a 7.1 inch (180 mm) bore diameter with 14.25 inch (362 mm) outside diameter and were fatigue cracked from longitudinal notches. The internal notches in all these specimens were 20 inches (508 mm) long, 1/4 inch (6.4 mm) deep, and 0.030 inch (0.762 mm) wide produced by electrical discharge machining. The external strains on the periphery at midsection of the cylinders were measured at crack depths of 1/4 inch (6.4 mm) to 3 inches (76 mm) measured from the bore, generally at intervals of 1/2 inch (13 mm) measured periodically by means of ultrasonic pulses reflected from the leading edge of the crack.

The gages were mounted circumferentially directly over each notch line. Strain measurements were made under static pressurization using a null-balancing technique. They were made on non-autofrettaged cylinders, and on autofrettaged cylinders of two different percent overstrain values. The percentage overstrain is the portion of the wall thickness which has exceeded the material yield strength during the prestressing by overpressurization.

The bore of the cylinder was partially filled with a cylindrical steel mandrel which supported the end closures, leaving the cylinder in essentially the open-end condition. A synthetic hydraulic oil was used as a pressurizing medium, filling the remainder of the cavity including the notches. Fatigue cracks grown from the initial notches were monitored for depth and shape with ultrasonics periodically as the cylinder was repeatedly pressurized from 4 ksi (28 MPa) to 48 ksi (330 MPa). The growth of fatigue cracks in cylinder

specimens is described by Throop⁴ and the 175 mm fatigue specimens, end packing, and ultrasonic crack-depth measurements are described by Davidson, et al.⁵

SPECIMEN AM2437B

We compared the fatigue behavior of the cylinders having multiple cracks with that of specimen AM2437B, a single-notch cylinder which had no auto-frettage overstrain. It was tested in an earlier investigation and failed at 1,500 cycles. The crack depth, a , versus number of cycles is plotted in Figure 1.

The crack propagation rate, da/dn , is plotted versus the crack depth, a , in Figure 2. The range of crack rate goes from 10^{-4} in./cycle at $a = 0.25$ inch to 10^{-2} in./cycle at $a = 1.3$ inch (33 mm) in a nearly linear manner on a log-log plot.

Figure 3 is a plot of the strain directly over the notch versus the crack depth. Starting at the theoretical strain of 1056 μ in./in. for the uncracked cylinder at 48,000 psi (330 MPa) pressure, it decreases to zero at the crack depth of 1.3 inch (33 mm), goes into compression briefly and then back sharply into tension as the ligament approaches failure at $N_f = 1,500$ cycles.

Compared to the curve for the approximation for a straight-fronted crack,

⁴Throop, J. F., "Fatigue Crack Growth in Thick-Walled Cylinders," Proceedings of National Conference on Fluid Power, XXVI, NCFP, Chicago, 1972, pp. 115-131.

⁵Davidson, T. E., Throop, J. F., and Reiner, A. N., "The Role of Fracture Toughness and Residual Stresses in the Fatigue and Fracture of Large Thick-Walled Pressure Vessels," Proceedings of National Conference on Fluid Power, XXVI, NCFP, Chicago, 1972, pp. 102-114.

which goes to zero strain at 0.85 inch (22 mm) crack depth, the graph shows the effect of the increasing curvature of the crack front.

Figure 4 shows how the crack front changed shape, particularly during the last cycle before firing.

SPECIMEN AM3244B

Specimen AM3244B with zero precent OS and dual notched 180 degrees apart endured 1,143 cycles. One of the notches grew a fatigue crack to 1.15 inch (29 mm) while the other notch only reached 0.65 inch (17 mm) as shown in Figure 5.

The faster crack went from a da/dn of 10^{-4} in./cycle at 1/4 inch (6.3 mm) depth to over 5×10^{-2} in./cycle at 1.15 inch (29 mm) depth as shown in Figure 6.

The strain over the deepest crack decreased from 1056 μ in./in. to zero at a crack depth of 1.18 inch (30 mm) as shown in Figure 7. The strain over the other crack decreased to 450 μ in./in. at 0.65 inch (17 mm), which put it on the curve for a straight-fronted crack. However, this crack ceased to grow beyond 0.65 inch (17 mm).

Figure 8 shows the change of shape of crack #1 and crack #2 in the last few cycles. Crack #2 perforated the wall with a 17 inch (432 mm) crack as shown.

SPECIMEN A2341B

Specimen A2341B was a four-notch cylinder with notches at zero degrees, 90 degrees, 180 degrees, and 270 degrees. All were 20 inches (0.5 m) long, 1.4 inch (6.3 mm) deep, and machined with a 30 mil EDM cutting tool. Crack #1

at zero degrees grew the fastest, as shown in the plot of crack depth versus number of cycles, Figure 9. Crack #3 at 180 degrees was nearly as fast, but did not go to failure, while crack #2 and crack #4 at 90 degrees and 270 degrees respectively, grew slowly and ceased to grow at a shallow depth.

Figure 9 shows that crack #1 grew continually at an ever increasing rate until failure occurred at 1,463 cycles. Cracks #3, #4, and #2 grew at lesser rates. The graph of da/dn versus crack depth in Figure 10 shows that crack #1 went from just under 10^{-4} in./cycle (2×10^{-6} m/cycle) to just under 10^{-1} in./cycle (2×10^{-3} m/cycle).

In Figure 11 the strain measured with a gage directly over the dominant crack decreased steadily from the Lame' strain for an uncracked cylinder until it reached zero strain at about 1.3 inch (33 mm) crack depth. It went negative for a short distance until it reached 1.4 inch (36 mm) crack depth when it went positive and the crack perforated the cylinder at 1,463 cycles. Figure 12 shows the final shape of the four cracks.

SPECIMEN MB3244B

Specimen MB3244B with 30 percent OS and dual notches 180 degrees apart endured 3,973 cycles, a factor of 3.5 times the number for zero percent overstrain. The graph of crack depth versus number of cycles is shown in Figure 13.

The crack rate went from 10^{-4} in./cycle (2.5×10^{-6} m/cycle) at 1/4 inch (6.3 mm) crack depth to 2×10^{-2} in./cycle (5×10^{-4} m/cycle) at three inches (76 mm) crack, with a plateau at about 1.6×10^{-4} in./cycle (4×10^{-6} m/cycle) between 0.3 and 0.5 inch (7.62 and 12.7 mm) crack depth, followed by a steep rise between 0.5 and 1.0 inch (12.7 and 25.4 mm) crack depth. This is the

rate of the faster crack, as shown in Figure 14. In Figure 15 the strain over crack #2 decreased from 1056 μ in./in. to zero at 1.23 inch (31.2 mm) crack depth. The strain over crack #1 decreased to 460 μ in./in. at 3,780 cycles and 0.90 inch (22.9 mm) crack depth.

In Figure 16 the change in shape during the last two hundred cycles is shown. Crack #1 grew a little, but crack #2 grew rapidly to perforate the wall.

SPECIMEN B2341B

Specimen B2341B is a dual-notch cylinder with 60 percent overstrain. We could not cause it to fail because of leaks in the end seals. The cracks were grown to 0.8 inch (20 mm) and 0.95 inch (24 mm) at 9,836 cycles. A reasonable extrapolation of the crack growth curve, as shown in Figure 17, would allow the fatigue life of the tube to be about 11,500 cycles, a factor of ten times the life of the non-autofrettaged dual-notch cylinder.

Figure 18 shows that when cracking was initiated it started increasing rapidly at first, followed by a plateau at 10^{-4} in./cycle (2.5×10^{-6} m/cycle) between 0.3 and 0.63 inch (7.6 and 16 mm) crack depth with a gradual rise to 2×10^{-4} in./cycle (5×10^{-6} m/cycle) as the crack grew toward one inch (25 mm) depth. Crack #1 followed crack #2 quite closely.

In Figure 19 the strains over the two notches were measured only to 8,650 cycles. Crack #2 had the largest decrease in strain with crack #1 following closely behind it. A reasonable extrapolation of the curve for crack #2 would estimate failure at 1.2 inch (30.5 mm) crack depth.

Figure 20 shows the crack shapes of the two cracks at the last observation. Neither crack had shown a tendency to become unstable and go to fast fracture yet.

DISCUSSION

Of the non-autofrettaged cylinders, the single-notch cylinder, AM2437B, had the longest fatigue life, followed by the four-notch cylinder, A2341B. The two-notch cylinder, AM3244B, had the shortest life. This had been predicted analytically for a straight-fronted crack, and was confirmed for curve-fronted cracks.

Of the multi-cracked cylinder, the fatigue lives are:

AM3244B	Two Cracks - 0% OS	1,143 cycles
A2341B	Four Cracks - 0% OS	1,463 cycles
MB3244B	Two Cracks - 30% OS	3,973 cycles
B2341B	Two Cracks - 60% OS	11,500 cycles - estimated

The advantage of autofrettage residual stress for internal cracks is readily apparent.

The cracks did not remain at equal depths in any of the multi-cracked tubes tested. On the contrary, one of the cracks became the dominant crack and grew to failure faster than the others.

The strain over the dominant crack decreases to zero in the same manner as for a single crack. The crack perforates the cylinder wall soon after the strain reduces to zero or becomes compressive.

CONCLUSIONS

1. Two opposing cracks in a cylinder give the fastest crack growth and shortest fatigue life.
2. Four equally spaced cracks are just about equivalent to the single-crack case.
3. Autofrettage residual stress from 30 percent OS increases the fatigue life over three times, and that from 60 percent OS increases the life over ten times that of the non-autofrettaged cylinder with the dual cracks.
4. Monitoring the circumferential strain on the outside wall over the dominant crack gives an indication of when failure is imminent.

REFERENCES

1. Throop, J. F. and Fujczak, R. R., "Strain Behavior of Pressurized Crack Thick-Walled Cylinders," *Experimental Mechanics*, The Society For Experimental Stress Analysis, August 1982, pp. 277-286.
2. Timoshenko, S. P. and Goodier, J. H., Theory of Elasticity, Third Edition, McGraw-Hill Book Company, New York, 1970, pp. 68-71.
3. Shannon, R. W. E., "Crack Growth Monitoring by Strain Sensing," *Pressure Vessels and Piping*, (1), Applied Science Publishing, Ltd., England, 1973, pp. 61-73.
4. Throop, J. F., "Fatigue Crack Growth in Thick-Walled Cylinders," *Proceedings of National Conference on Fluid Power*, XXVI, NCFP, Chicago, 1972, pp. 113-131.
5. Davidson, T. E., Throop, J. F., and Reiner, A. N., "The Role of Fracture Toughness and Residual Stresses in the Fatigue and Fracture of Large Thick-Walled Pressure Vessels," *Proceedings of National Conference on Fluid Power*, XXVI, NCFP, Chicago, 1972, pp. 102-114.

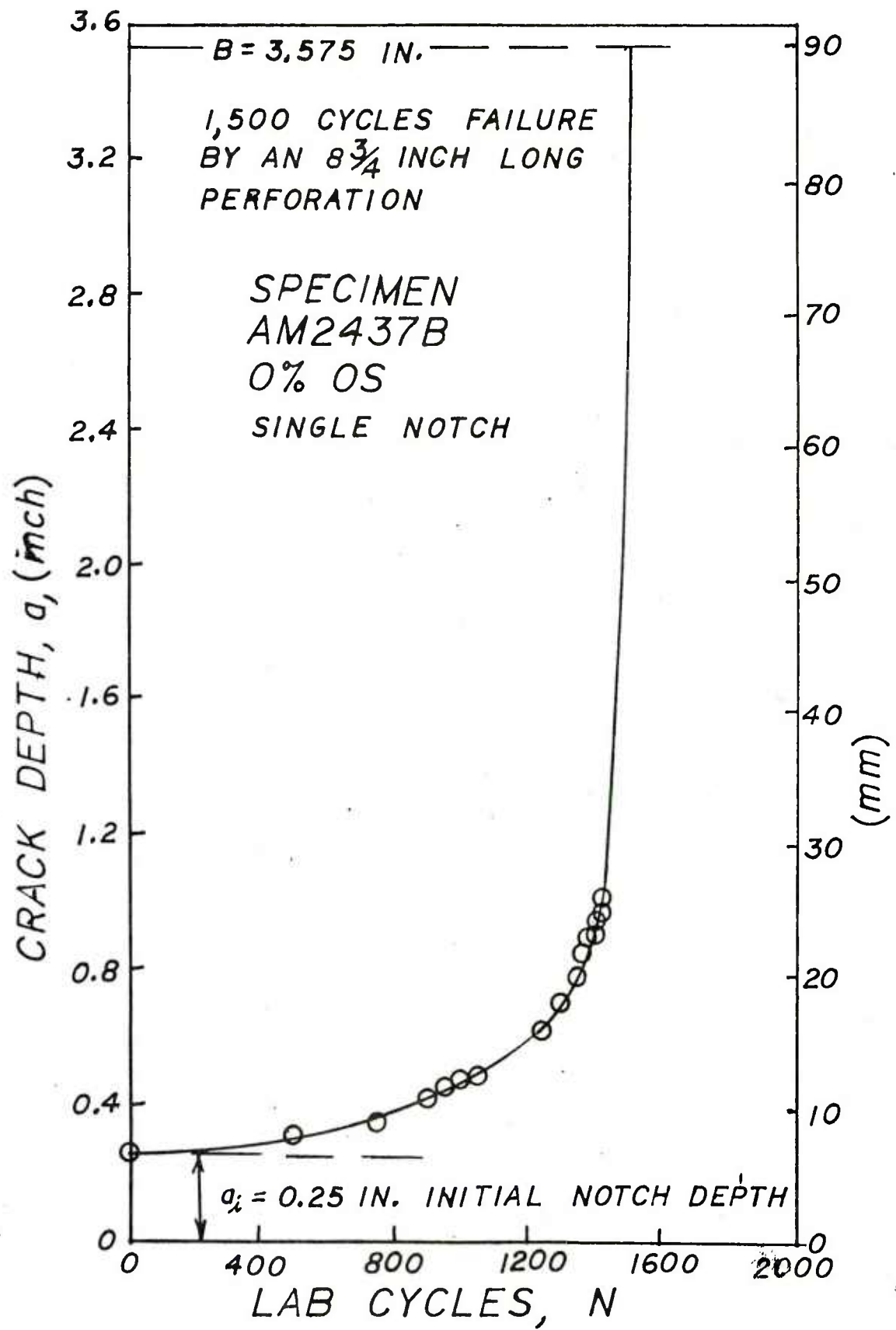


Figure 1. Crack depth, a , versus number of cycles.

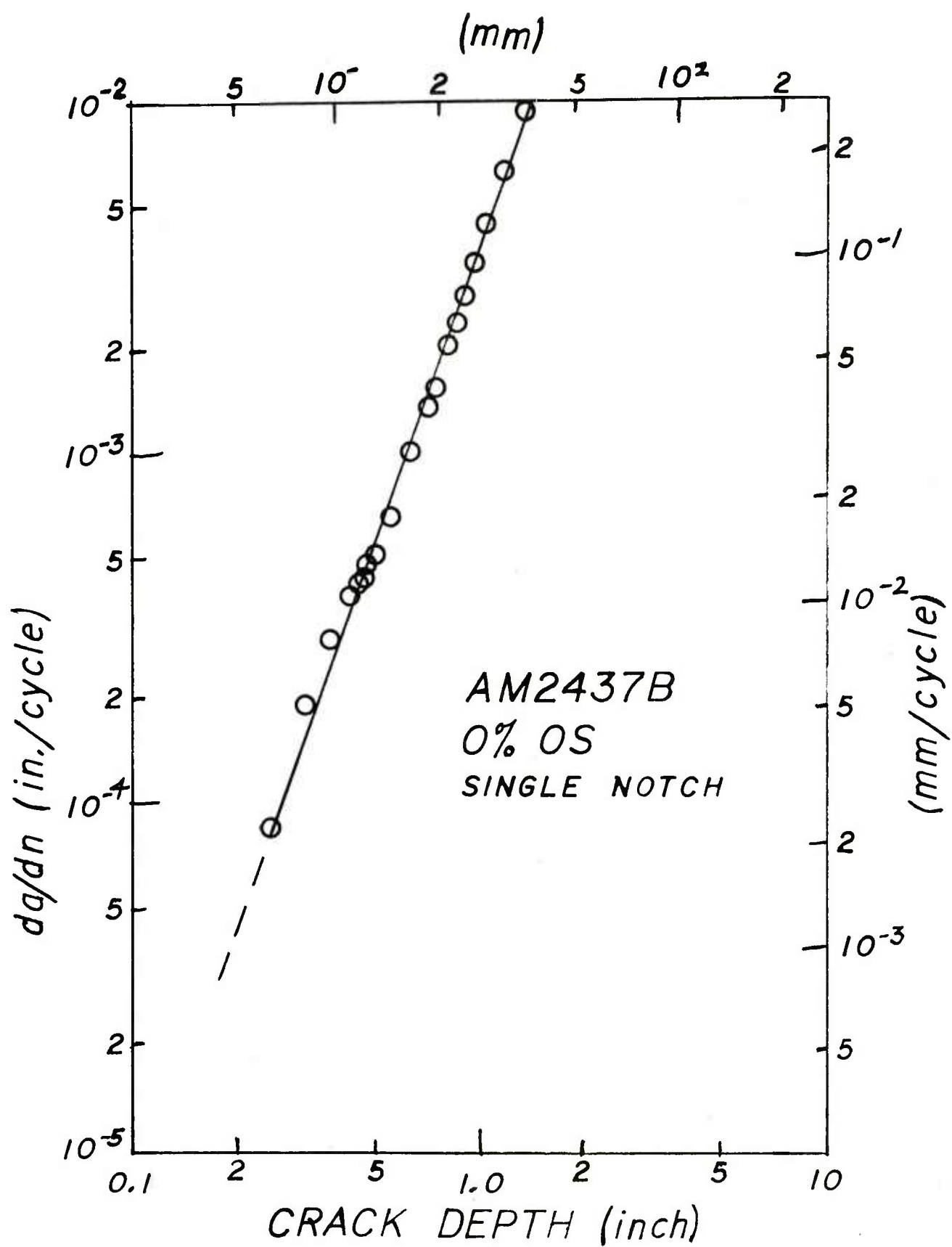


Figure 2. Crack propagation rate versus crack depth, a .

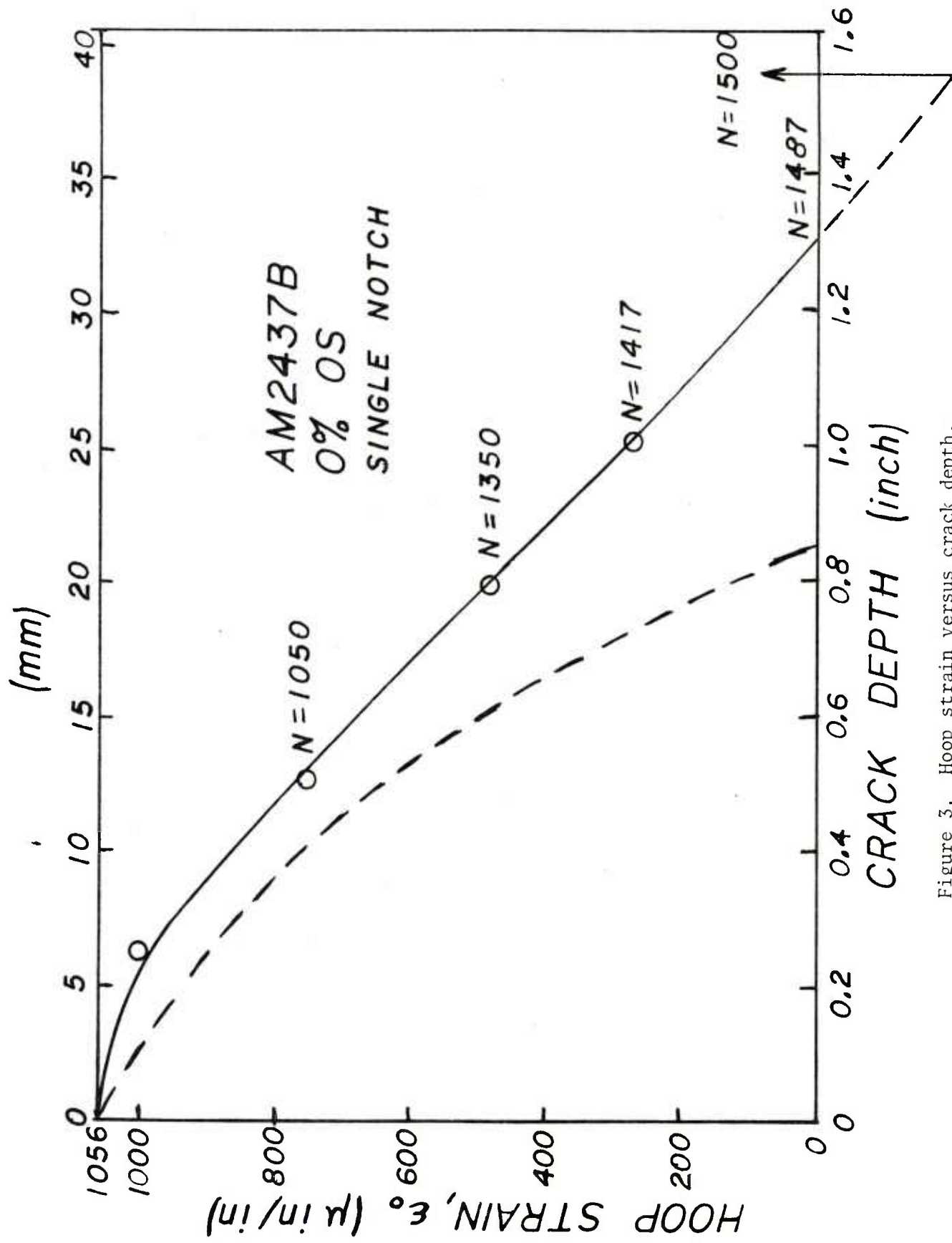


Figure 3. Hoop strain versus crack depth.

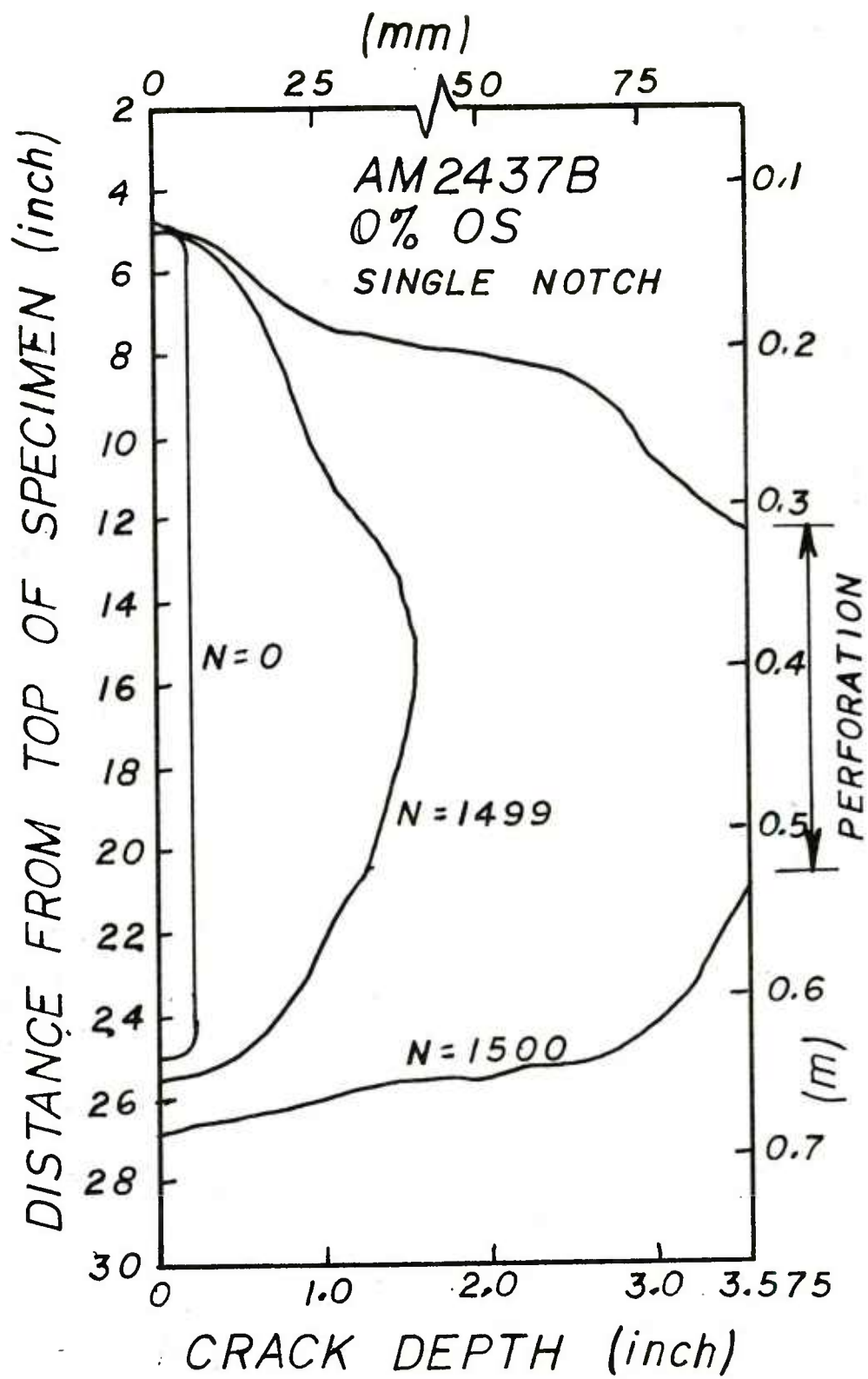


Figure 4. Crack front shape change before failure.

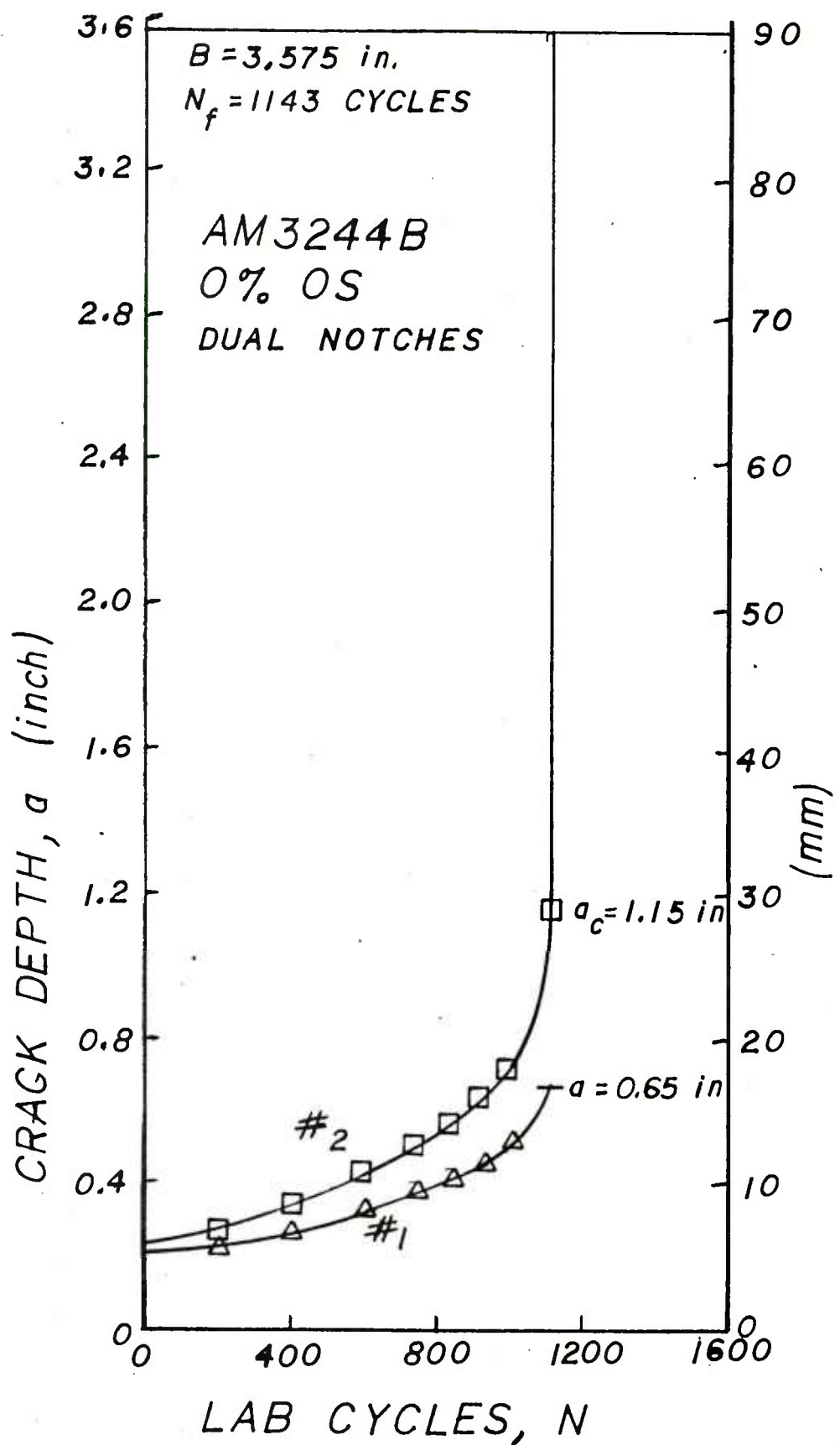


Figure 5. Comparison of dual notches, 180 degrees apart after 1143 cycles.

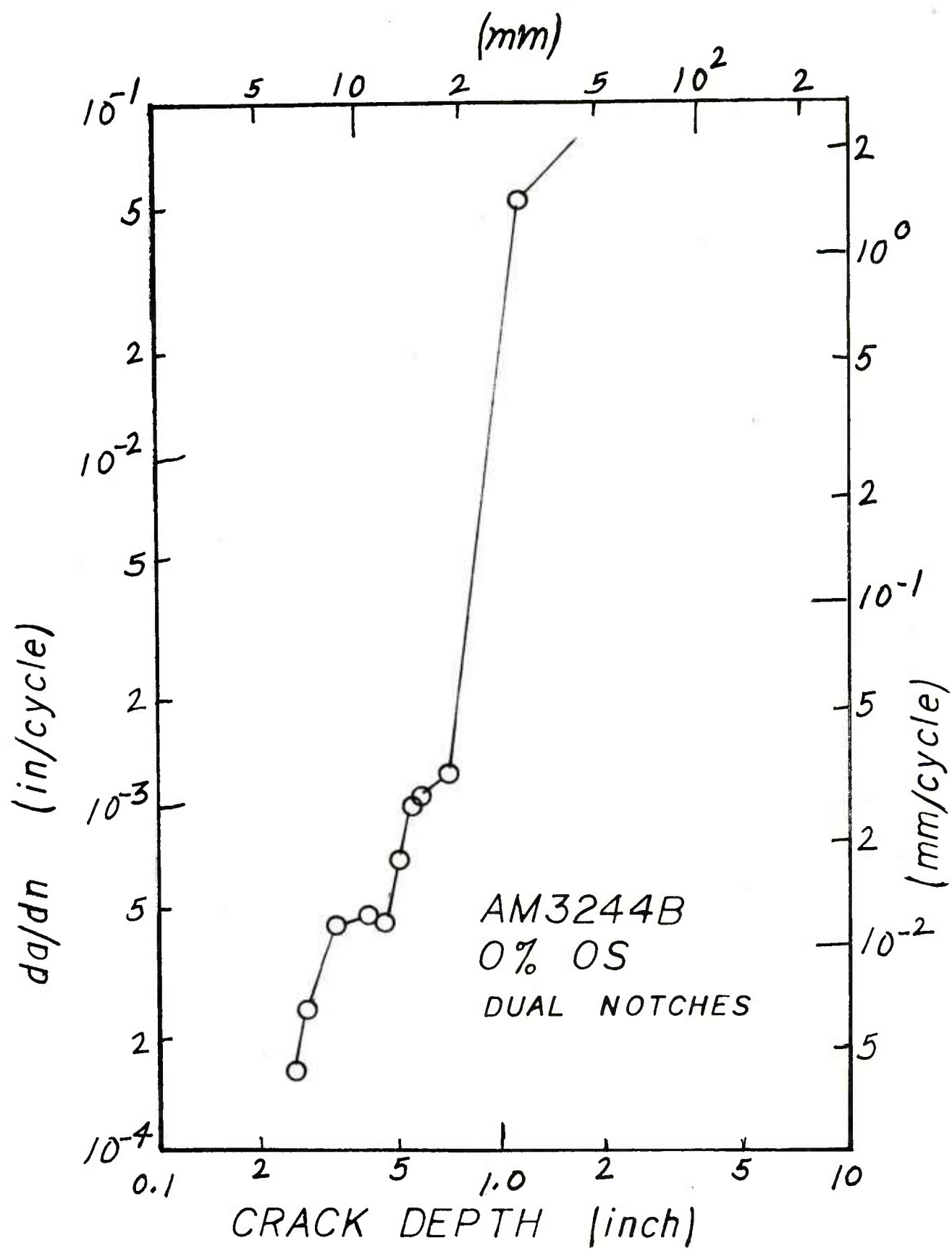


Figure 6. Crack propagation rate versus crack depth for dual notches.

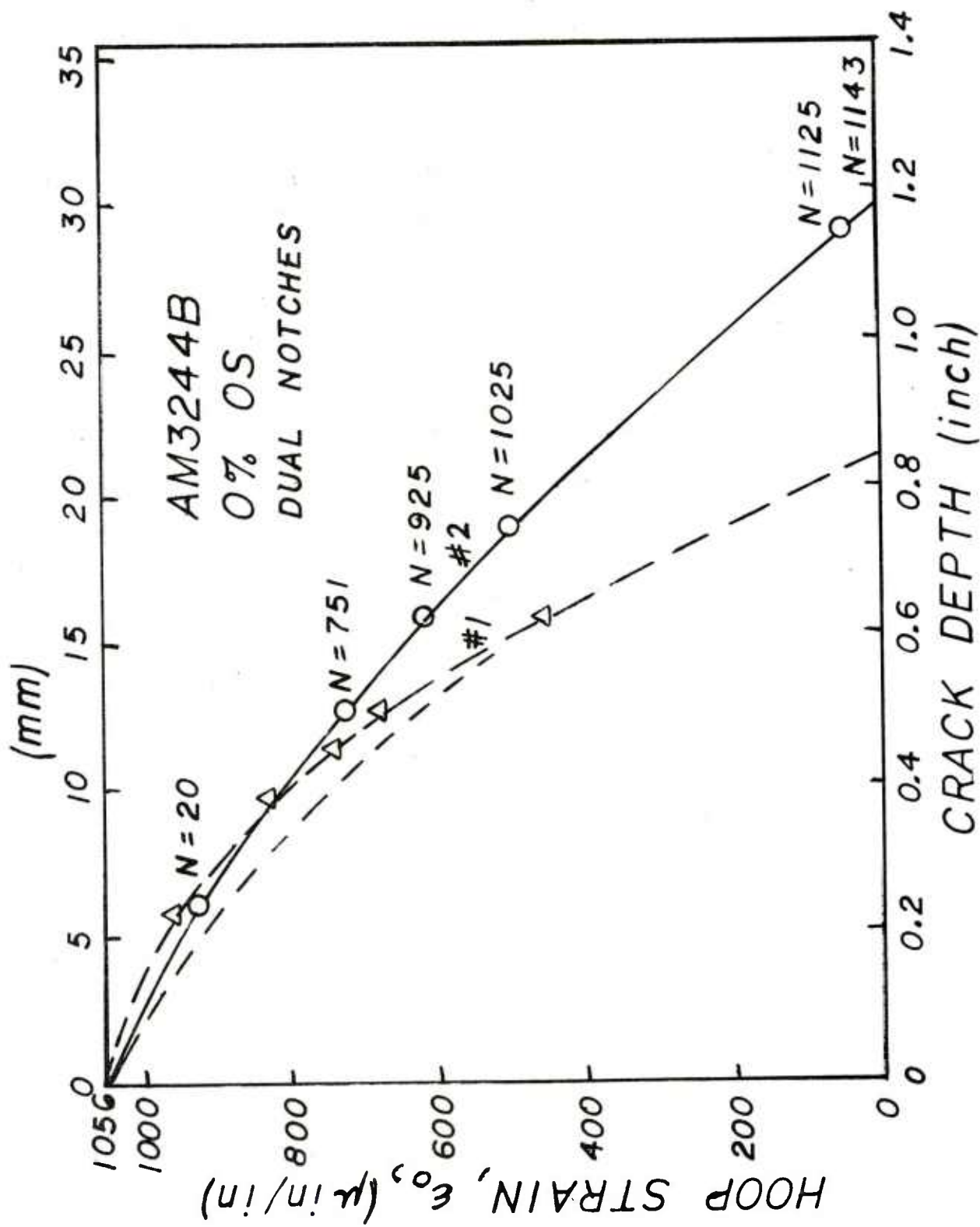


Figure 7. Comparison of hoop strain for dual notches.

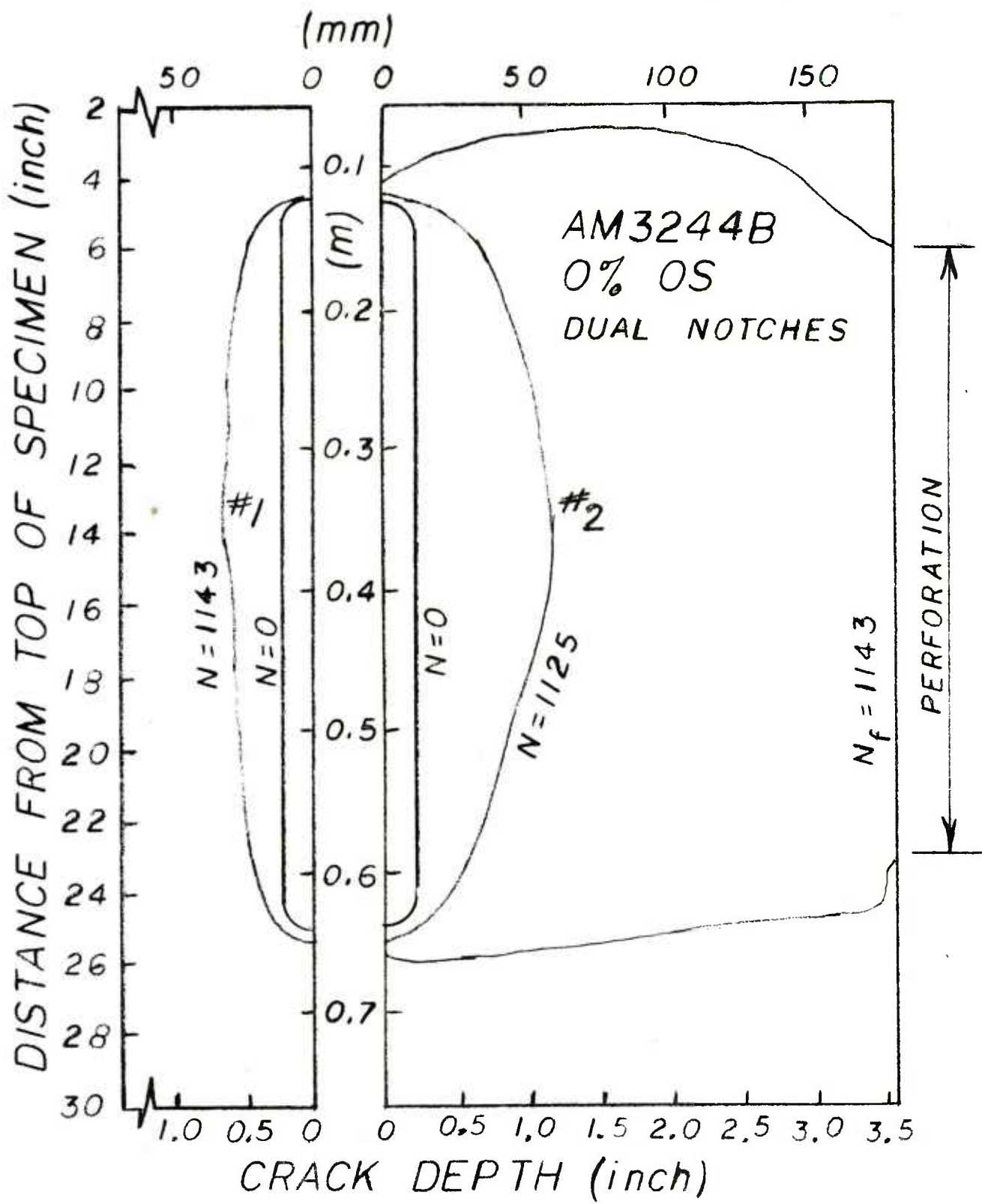


Figure 8. Changes in shapes of crack #1 and crack #2 during last few cycles.

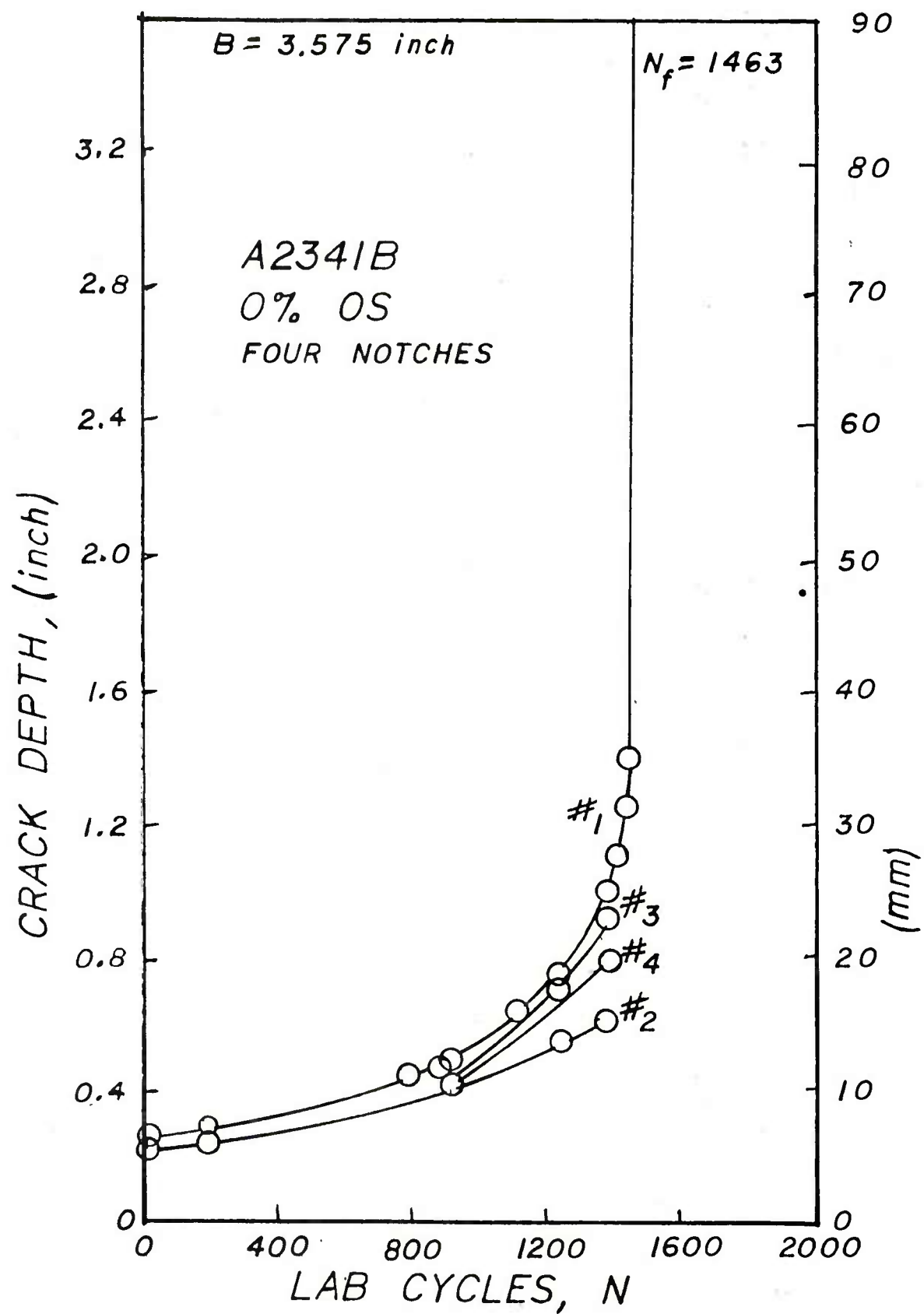


Figure 9. Crack depth versus number of cycles for four cracks.

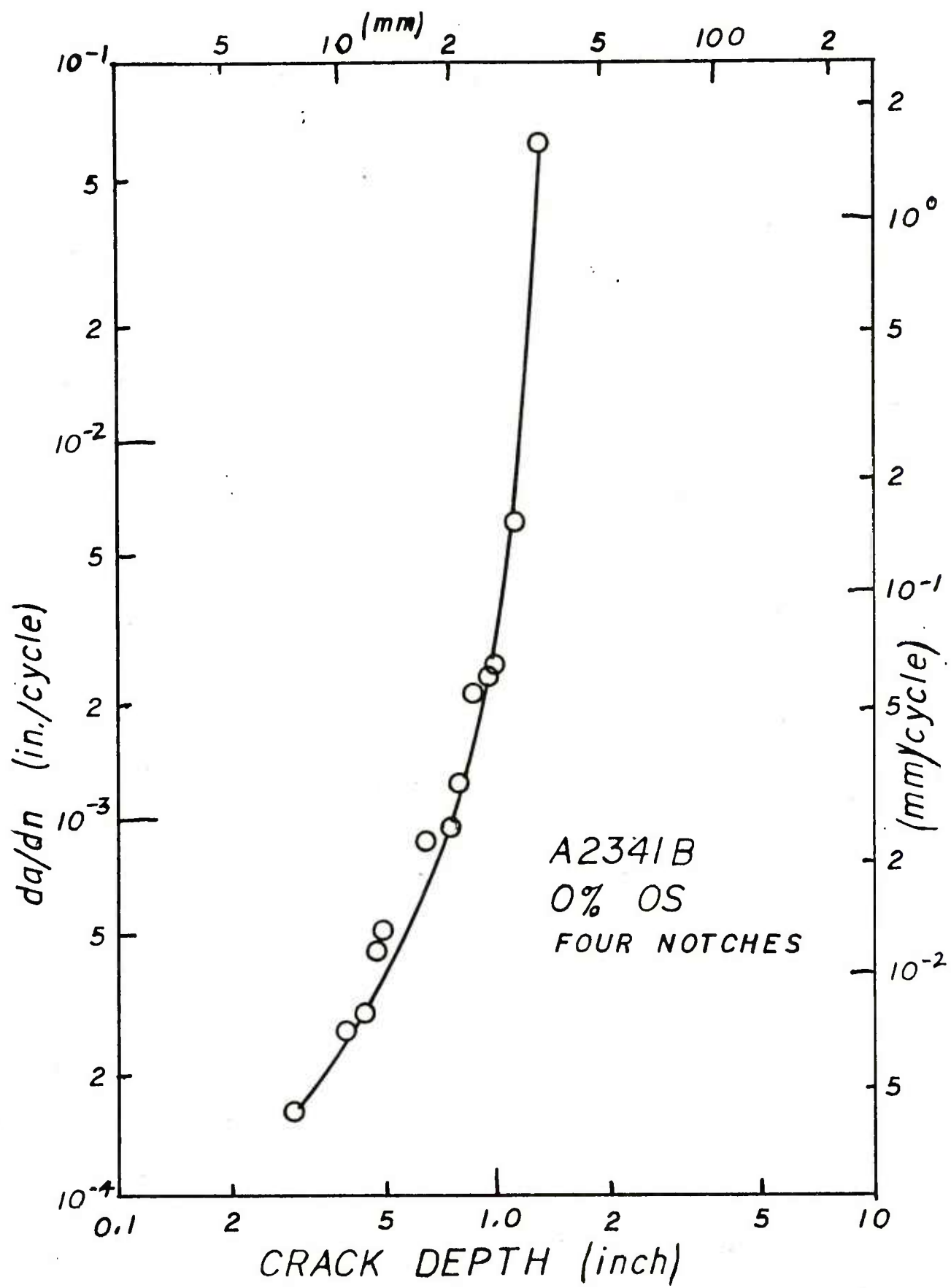


Figure 10. Graph of da/dn versus crack depth for crack #1.

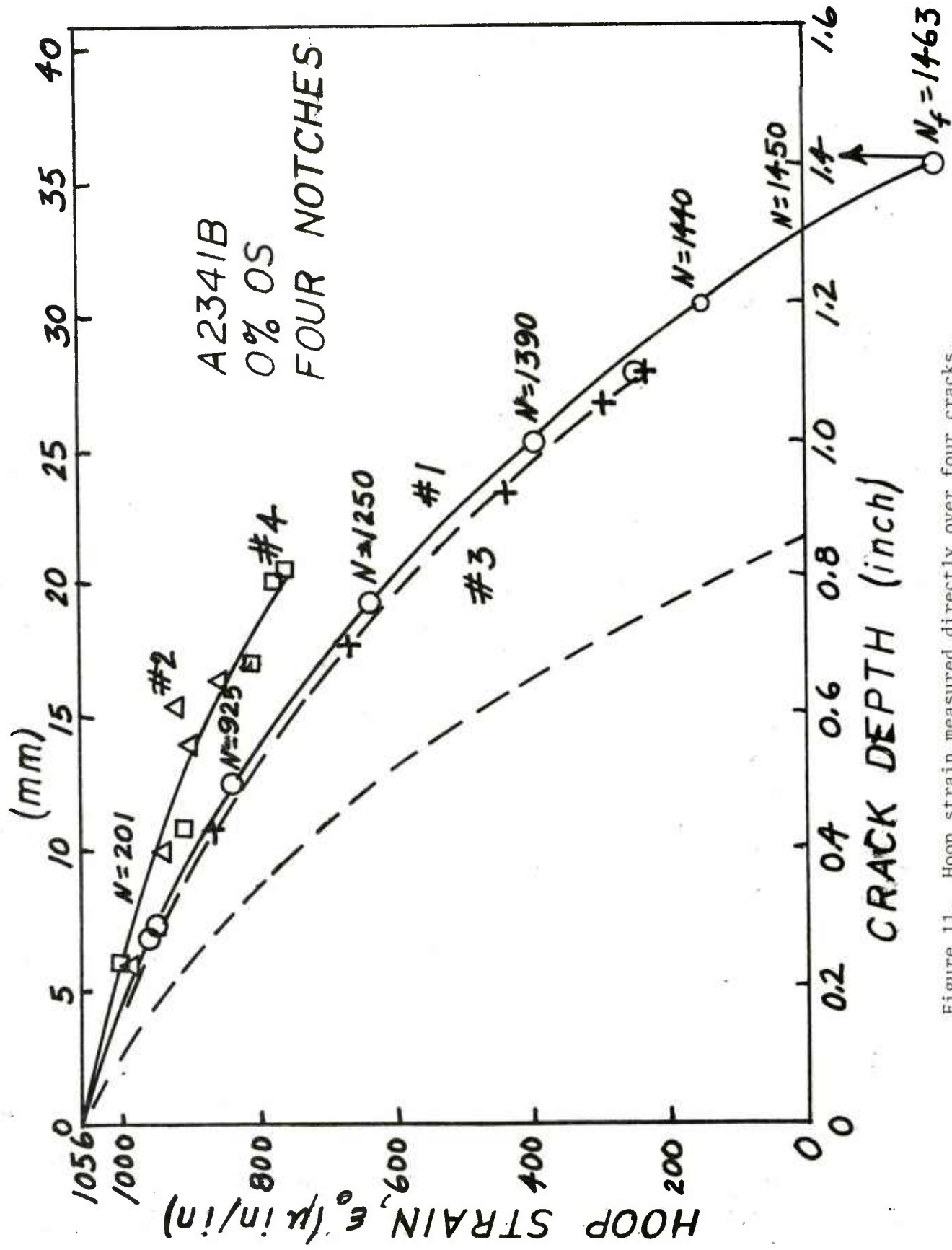


Figure 11. Hoop strain measured directly over four cracks.

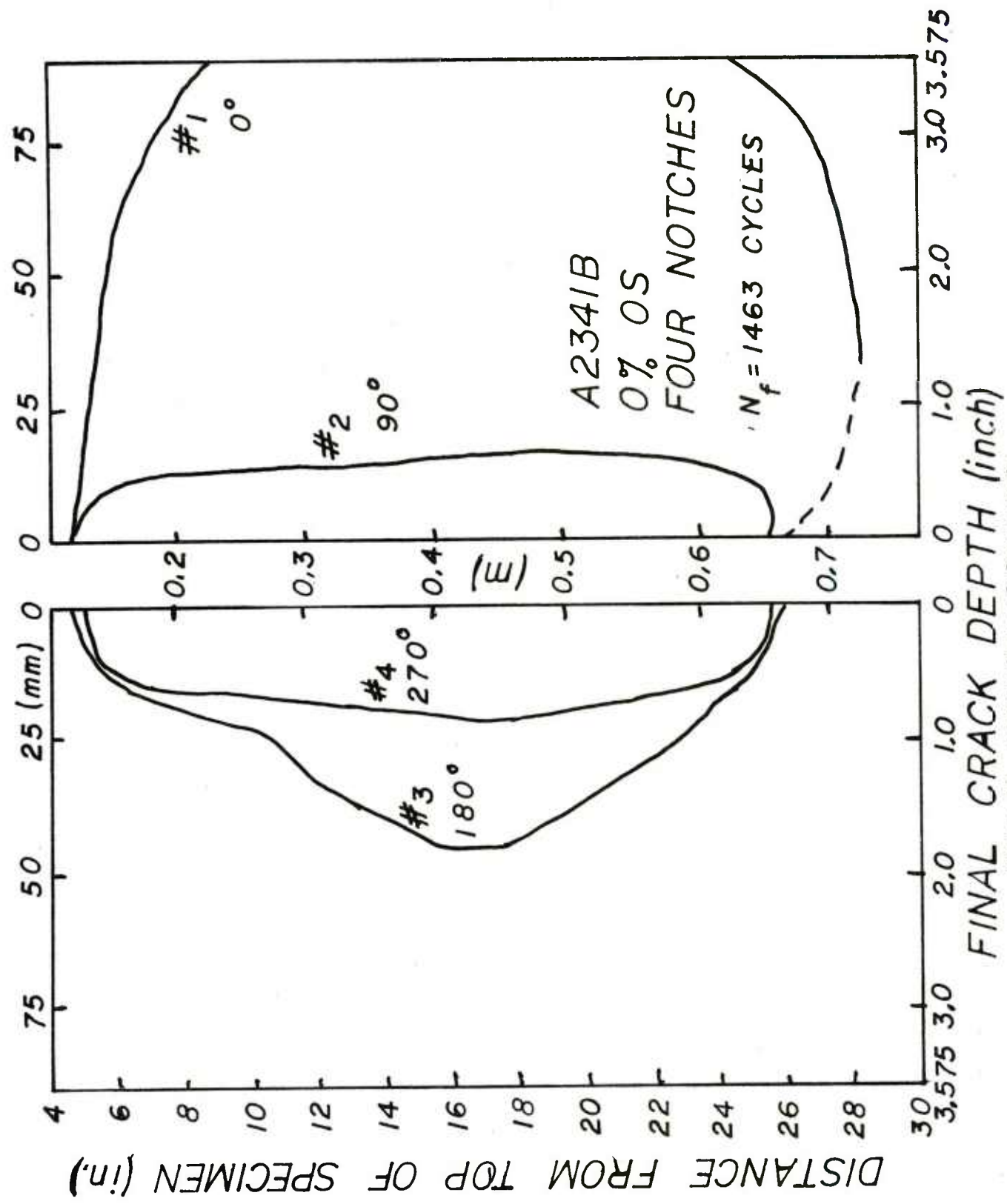


Figure 12. Final shape of four cracks.

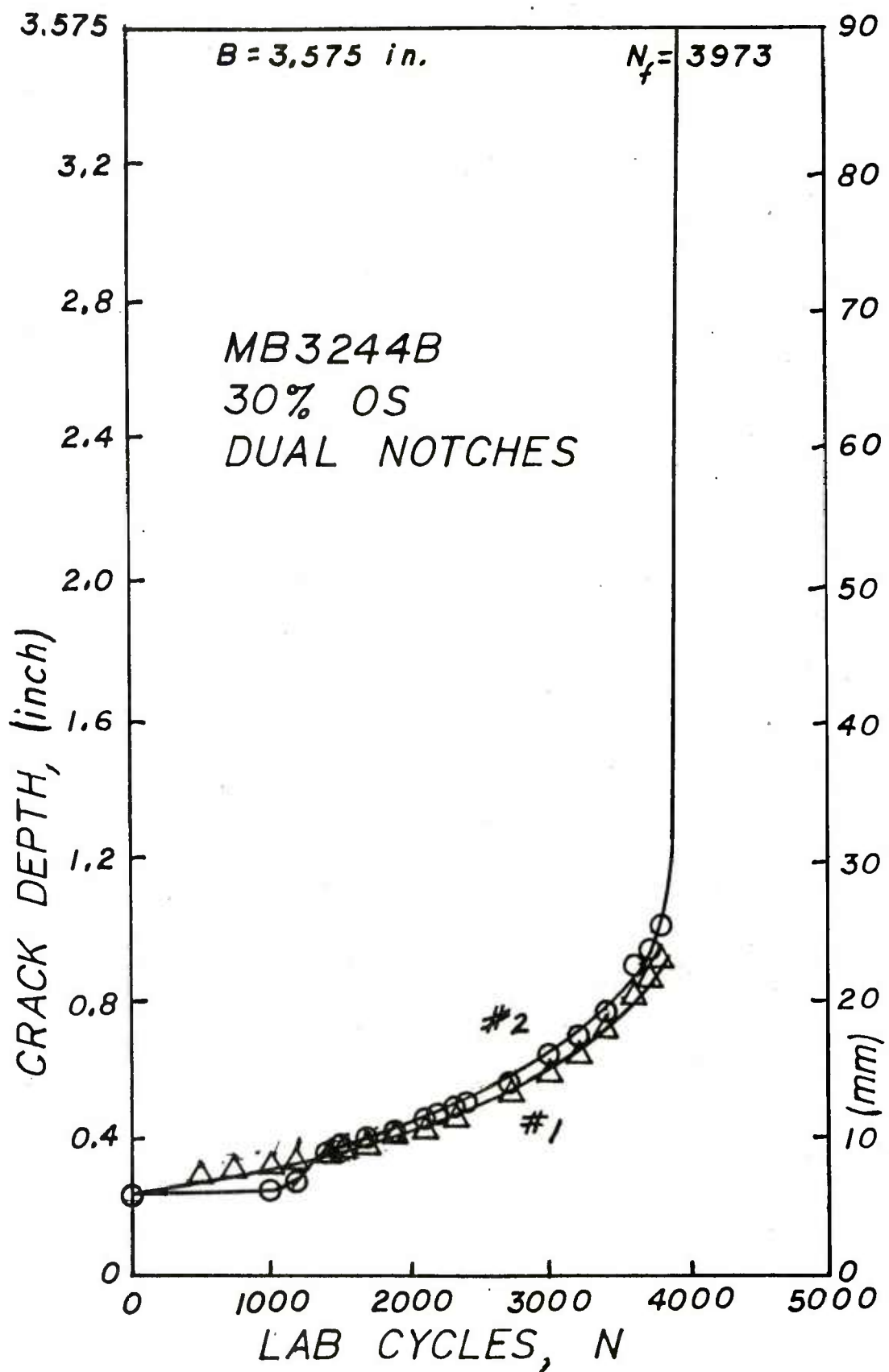


Figure 13. Crack depth versus number of cycles for dual notches, 30 percent overstrain.

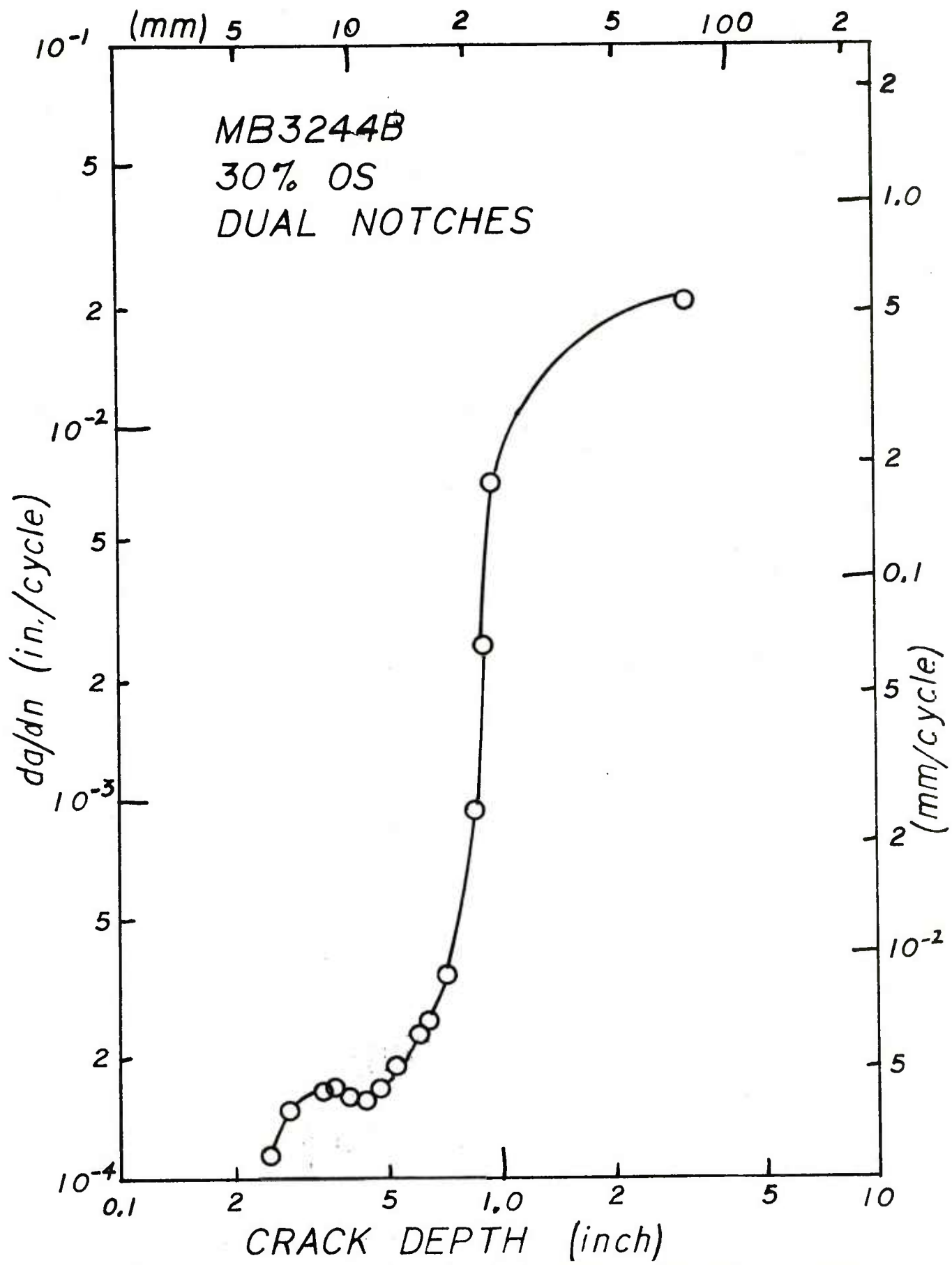


Figure 14. da/dn versus crack depth for dual notches, 30 percent overstrain.

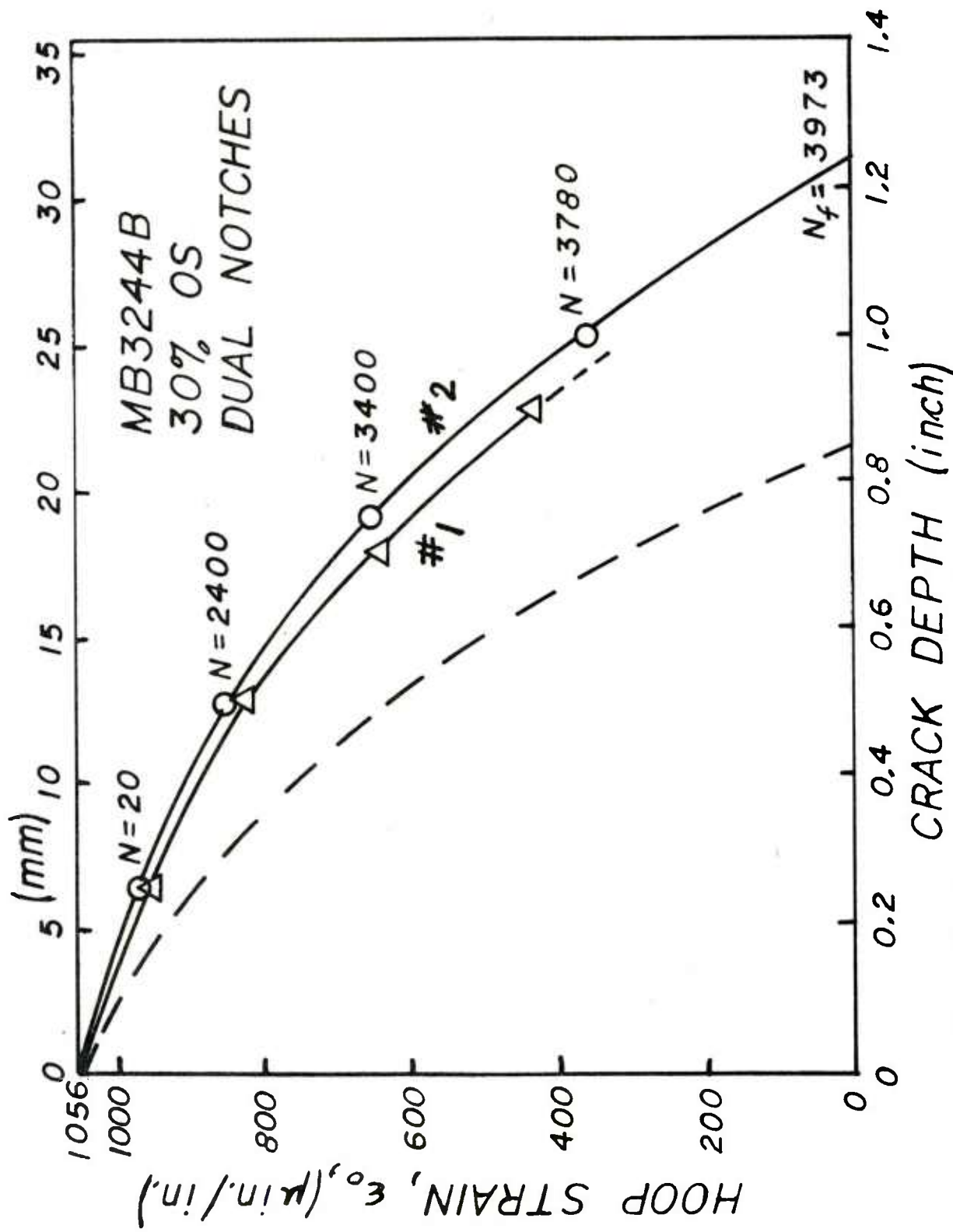


Figure 15. Hoop strain versus crack depth for dual notches, 30 percent overstrain.

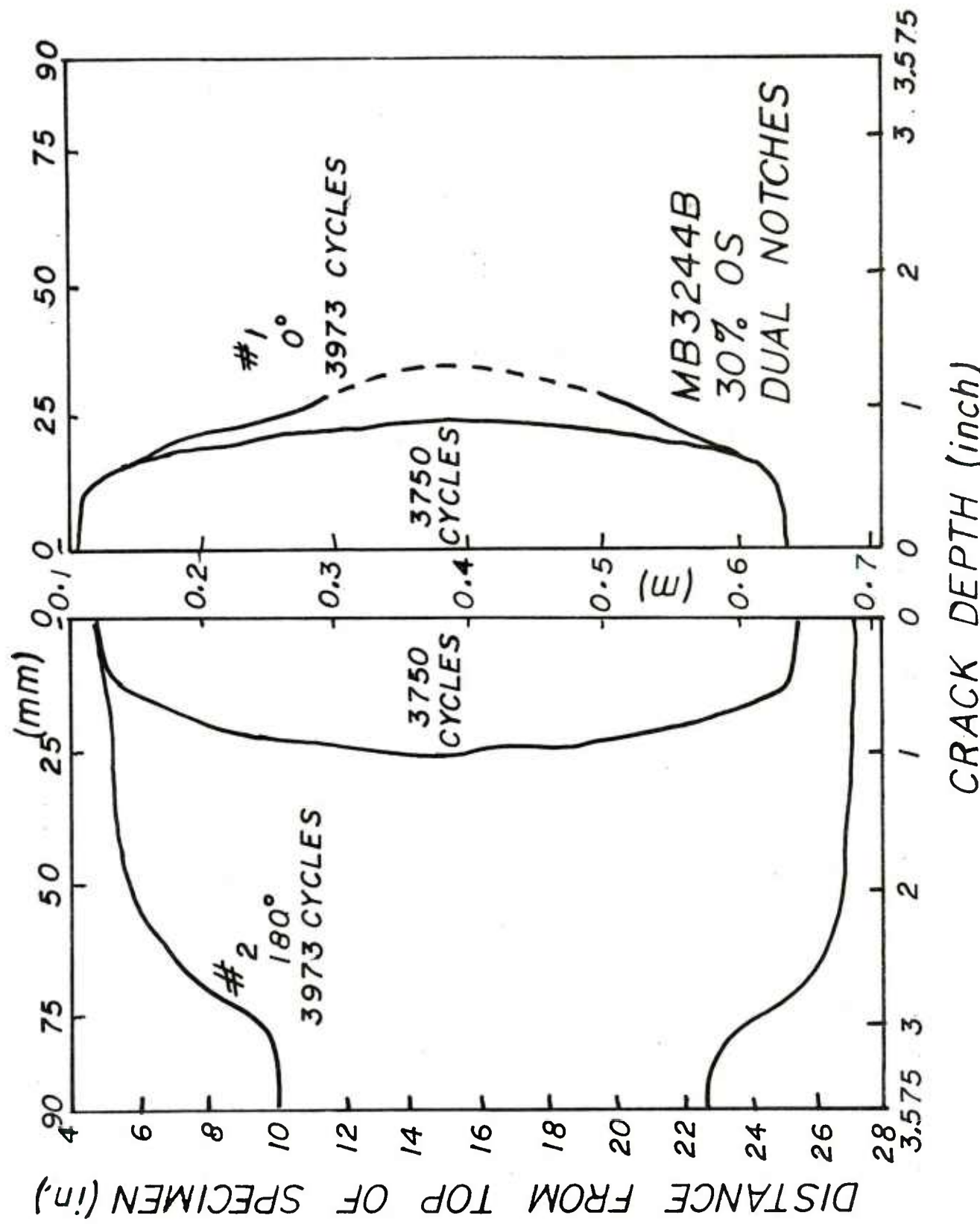


Figure 16. Changes in shapes of crack #1 and crack #2 from dual notches, 30 percent overstrain, during final 200 cycles.

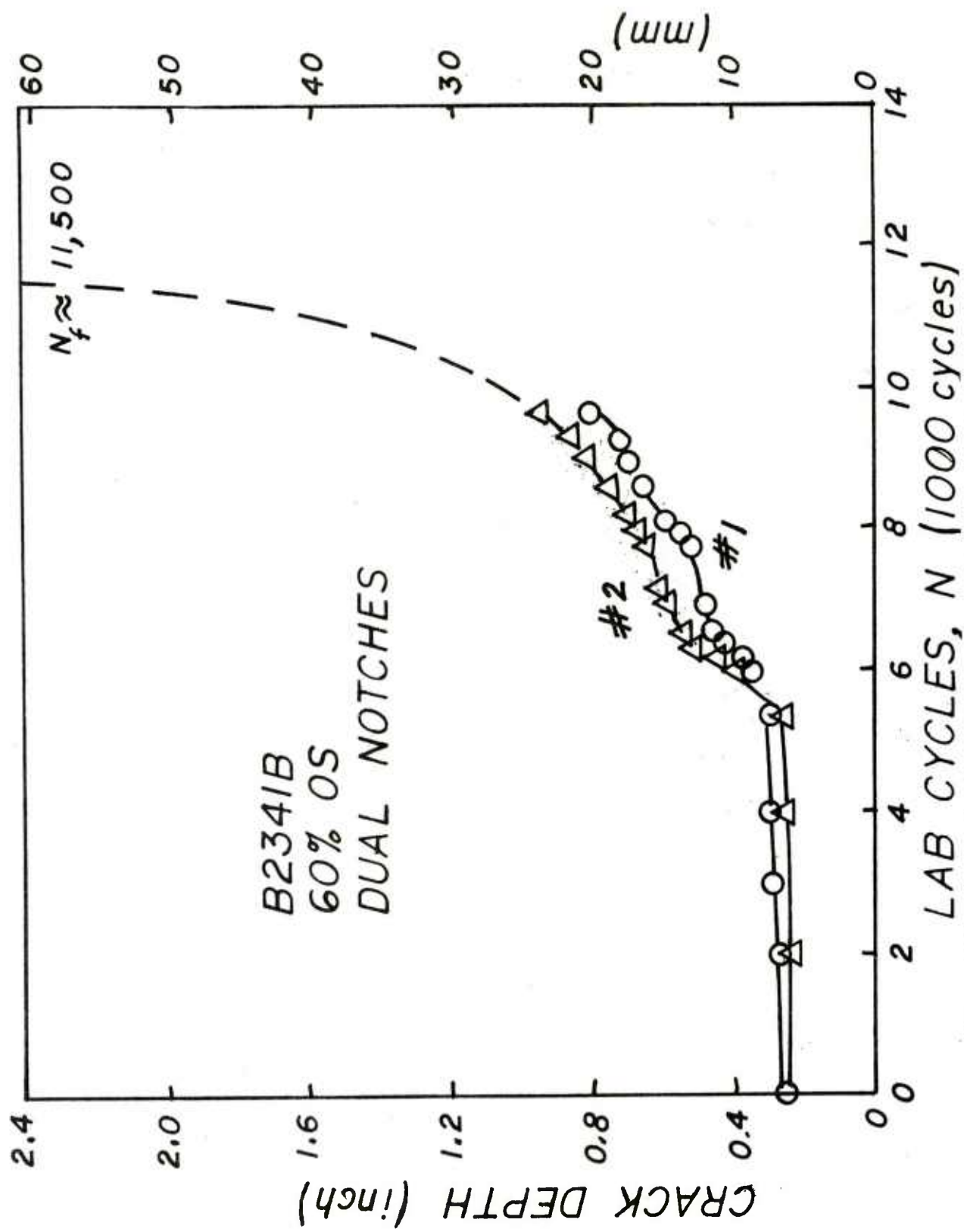


Figure 17. Crack depth versus number of cycles for dual notches, 60 percent overstrain,

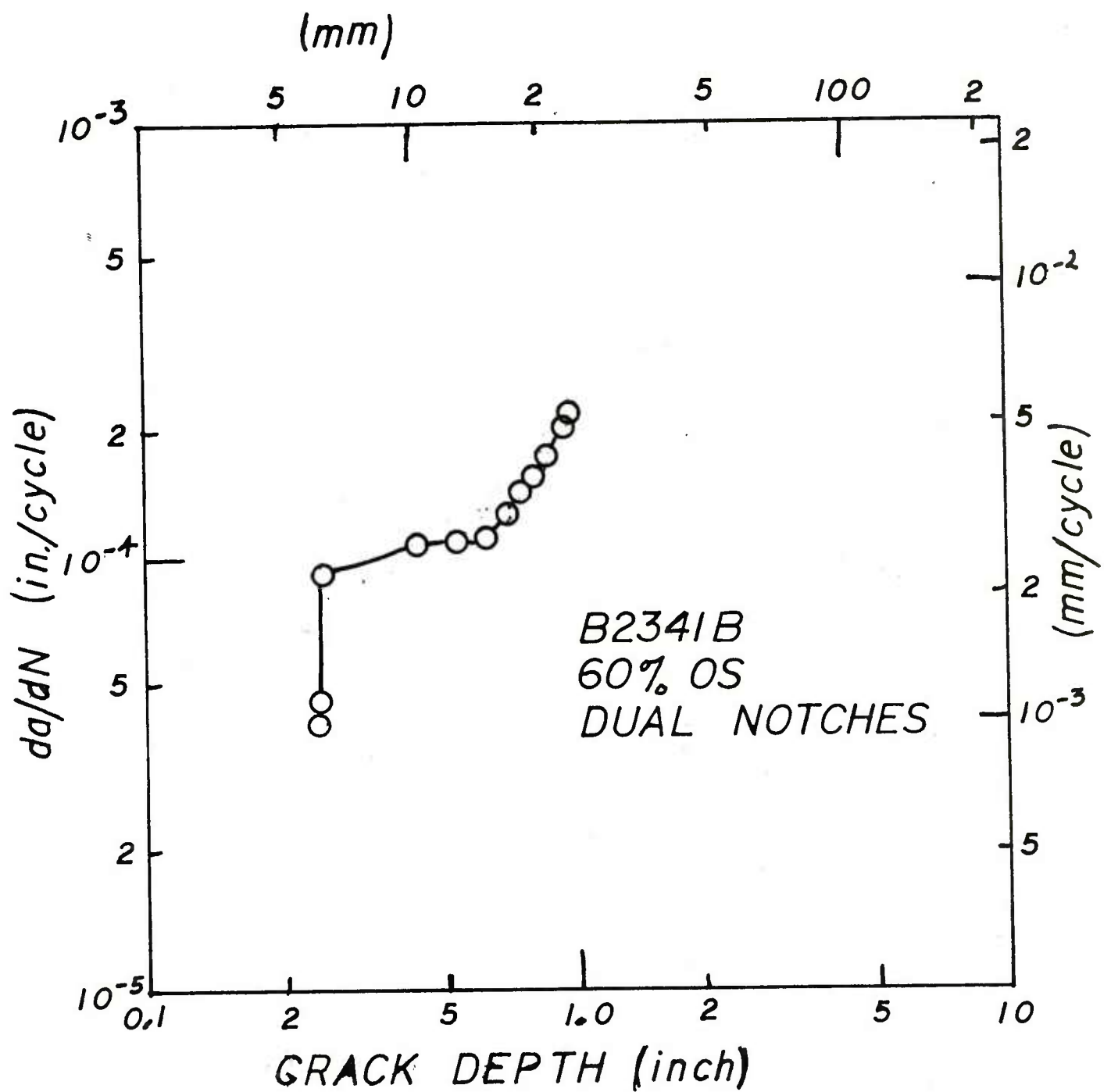


Figure 18. da/dn versus crack depth for dual notches, 60 percent overstrain.

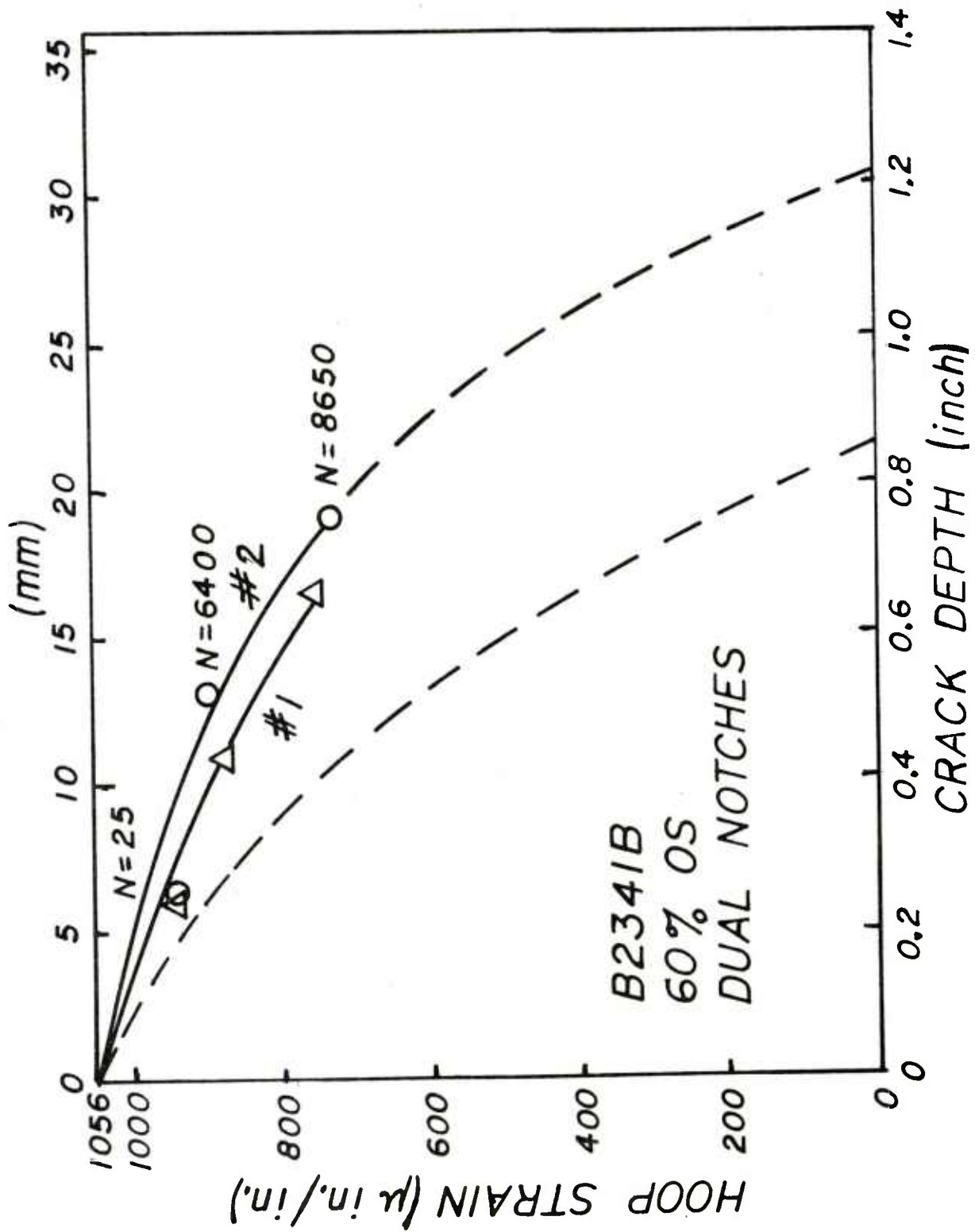


Figure 19. Hoop strain versus crack depth for dual notches, 60 percent overstrain.

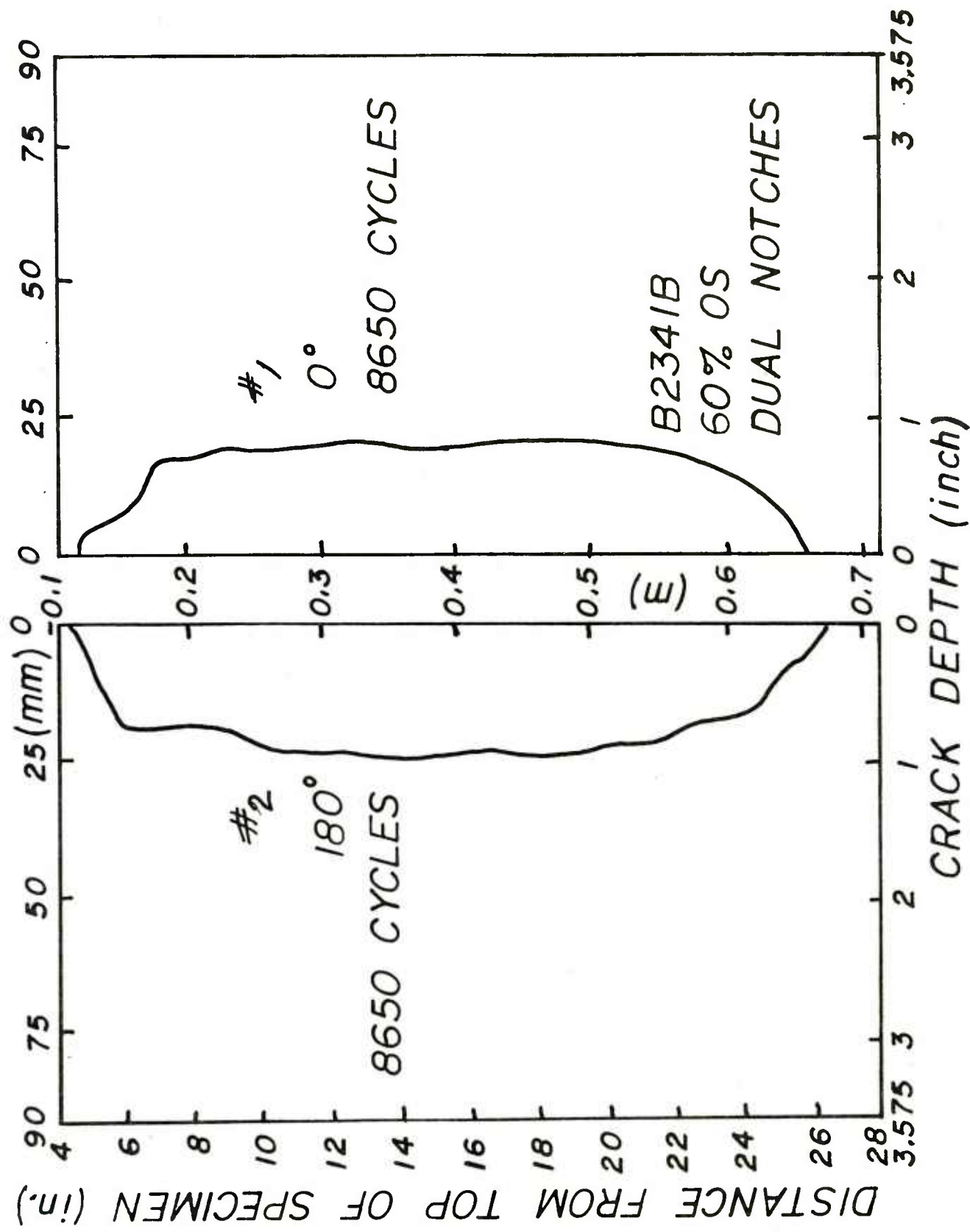


Figure 20. Final crack shapes for dual notches, 60 percent overstrain.

TECHNICAL REPORT INTERNAL DISTRIBUTION LIST

	<u>NO. OF COPIES</u>
CHIEF, DEVELOPMENT ENGINEERING BRANCH	
ATTN: DRSMC-LCB-D	1
-DP	1
-DR	1
-DS (SYSTEMS)	1
-DS (ICAS GROUP)	1
-DC	1
CHIEF, ENGINEERING SUPPORT BRANCH	
ATTN: DRSMC-LCB-S	1
-SE	1
CHIEF, RESEARCH BRANCH	
ATTN: DRSMC-LCB-R	2
-R (ELLEN FOGARTY)	1
-RA	1
-RM	1
-RP	1
-RT	1
TECHNICAL LIBRARY	5
ATTN: DRSMC-LCB-TL	
TECHNICAL PUBLICATIONS & EDITING UNIT	2
ATTN: DRSMC-LCB-TL	
DIRECTOR, OPERATIONS DIRECTORATE	1
DIRECTOR, PROCUREMENT DIRECTORATE	1
DIRECTOR, PRODUCT ASSURANCE DIRECTORATE	1

NOTE: PLEASE NOTIFY DIRECTOR, BENET WEAPONS LABORATORY, ATTN: DRSMC-LCB-TL, OF ANY ADDRESS CHANGES.

TECHNICAL REPORT EXTERNAL DISTRIBUTION LIST

<u>NO. OF COPIES</u>	<u>NO. OF COPIES</u>		
ASST SEC OF THE ARMY RESEARCH & DEVELOPMENT ATTN: DEP FOR SCI & TECH THE PENTAGON WASHINGTON, D.C. 20315	1	COMMANDER US ARMY AMCCOM ATTN: DRSMC-LEP-L(R) ROCK ISLAND, IL 61299	1
COMMANDER DEFENSE TECHNICAL INFO CENTER ATTN: DTIC-DDA CAMERON STATION ALEXANDRIA, VA 22314	12	COMMANDER ROCK ISLAND ARSENAL ATTN: SMCR-ENM (MAT SCI DIV) ROCK ISLAND, IL 61299	1
COMMANDER US ARMY MAT DEV & READ COMD ATTN: DRCDE-SG 5001 EISENHOWER AVE ALEXANDRIA, VA 22333	1	DIRECTOR US ARMY INDUSTRIAL BASE ENG ACTV ATTN: DRXIB-M ROCK ISLAND, IL 61299	1
COMMANDER ARMAMENT RES & DEV CTR US ARMY AMCCOM ATTN: DRSMC-LC(D) DRSMC-LCE(D) DRSMC-LCM(D) (BLDG 321) DRSMC-LCS(D) DRSMC-LCU(D) DRSMC-LCW(D) DRSMC-SCM-O (PLASTICS TECH EVAL CTR, BLDG. 351N) DRSMC-TSS(D) (STINFO) DOVER, NJ 07801	1 1 1 1 1 1 1 1 2	COMMANDER US ARMY TANK-AUTMV R&D COMD ATTN: TECH LIB - DRSTA-TSL WARREN, MI 48090	1
SEARCH LABORATORY RCH & DEV CTR 1 SB-S (STINFO) NG GROUND, MD 21005	1	COMMANDER US ARMY TANK-AUTMV COMD ATTN: DRSTA-RC WARREN, MI 48090	1
MS ANALYSIS ACTV P NG GROUND, MD 21005	1	COMMANDER US MILITARY ACADEMY ATTN: CHMN, MECH ENGR DEPT WEST POINT, NY 10996	1
NOTIFY COMMANDER, ARMAMENT RESEARCH AND DEVELOPMENT CENTER, AMCCOM, ATTN: BENET WEAPONS LABORATORY, DRSMC-LCB-TL, ALBANY, NY 12189, OF ANY ADDRESS CHANGES.		US ARMY MISSILE COMD REDSTONE SCIENTIFIC INFO CTR ATTN: DOCUMENTS SECT, BLDG. 4484 REDSTONE ARSENAL, AL 35898	2
		COMMANDER US ARMY FGN SCIENCE & TECH CTR ATTN: DRXST-SD 220 7TH STREET, N.E. CHARLOTTESVILLE, VA 22901	1

TECHNICAL REPORT EXTERNAL DISTRIBUTION LIST (CONT'D)

	<u>NO. OF COPIES</u>		<u>NO. OF COPIES</u>
COMMANDER US ARMY MATERIALS & MECHANICS RESEARCH CENTER ATTN: TECH LIB - DRXMR-PL WATERTOWN, MA 01272	2	DIRECTOR US NAVAL RESEARCH LAB ATTN: DIR, MECH DIV CODE 26-27, (DOC LIB) WASHINGTON, D.C. 20375	1
COMMANDER US ARMY RESEARCH OFFICE ATTN: CHIEF, IPO P.O. BOX 12211 RESEARCH TRIANGLE PARK, NC 27709	1	COMMANDER AIR FORCE ARMAMENT LABORATORY ATTN: AFATL/DLJ AFATL/DLJG EGLIN AFB, FL 32542	1
COMMANDER US ARMY HARRY DIAMOND LAB ATTN: TECH LIB 2800 POWDER MILL ROAD ADELPHIA, MD 20783	1	METALS & CERAMICS INFO CTR BATTELLE COLUMBUS LAB 505 KING AVENUE COLUMBUS, OH 43201	1
COMMANDER NAVAL SURFACE WEAPONS CTR ATTN: TECHNICAL LIBRARY CODE X212 DAHLGREN, VA 22448	1		

NOTE: PLEASE NOTIFY COMMANDER, ARMAMENT RESEARCH AND DEVELOPMENT CENTER,
US ARMY AMCCOM, ATTN: BENET WEAPONS LABORATORY, DRSMC-LCB-TL,
WATERVLIET, NY 12189, OF ANY ADDRESS CHANGES.

READER EVALUATION

Please take a few minutes to complete the questionnaire below and mail it to the following address: Commander, Armament Research and Development Center, U.S. Army AMCCOM, ATTN: Technical Publications, DRSMC-LC, Watervliet, NY 12189.

1. Benet Weapons Lab. Report Number _____
2. Please evaluate this publication (check off one or more as applicable).

Information Relevant	_____	_____
Information Technically Satisfactory	_____	_____
Format Easy to Use	_____	_____
Overall, Useful to My Work	_____	_____
Other Comments	_____	

3. Has the report helped you in your own areas of interest? (i.e. preventing duplication of effort in the same or related fields, savings of time, or money).

4. How is the report being used? (Source of ideas for new or improved designs. Latest information on current state of the art, etc.).

5. How do you think this type of report could be changed or revised to improve readability, usability?

6. Would you like to communicate directly with the author of the report regarding subject matter or topics not covered in the report? If so please fill in the following information.

Name : _____

Telephone Number: _____

Organization Address: _____